Molecular Dynamics Simulation of Immobilized Artifical Membranes

Qing Sheng and Klaus Schulten*

Department of Physics and Beckman Institute, University of Illinois at Urbana-Champaign, Urbana, Illinois 61801

Charles Pidgeon

Department of Medicinal Chemistry and Pharmacognosy, School of Pharmacy, Purdue University, West Lafayette, Illinois 47907

Received: January 13, 1995; In Final Form: April 4, 1995[⊗]

A 250 ps molecular dynamics (MD) simulation of an immobilized artificial membrane (IAM) surface was performed and compared to previous MD simulations of fluid membranes. Experimentally, IAM surfaces are prepared by immobilizing monolayers of membrane lipids and, consequently, IAM surfaces are distinct from the surfaces found in fluid membranes. The computer-generated IAM surface used for the simulation contained 36 phosphatidylcholine (PC) molecules and 2487 water molecules. In addition, seven straight chain alkanes were intercalated between the 36 PC molecules to simulate the experimental end capping performed during the synthesis of IAMs. The interfacial distributions of glycerol phosphocholine atoms were compared for both immobilized and fluid membranes. MD simulations indicate that the distribution of glycerol phosphocholine atoms is virtually identical in both fluid and immobilized membranes. This indicates that the polar interfacial region of the IAM surface is very similar to the polar interfacial region of fluid membranes. Water molecules are strongly polarized at the IAM interfacial region. Water polarization decays experimentally from the first hydration layer to bulk water with a decay length of 13 Å. Water did not penetrate into the hydrophobic alkyl chains of the IAM interphase during the 250 ps simulation. Water diffusion near the glycerolphosphocholine head groups, calculated from the 250 ps simulation, is twice as fast in the plane of the membrane as compared to the direction that is normal to the membrane. The internal phosphate diffusion constant calculated from a 250 ps trajectory was 1.7 ns^{-1} which is similar to the value of 1 ns^{-1} experimentally determined by NMR. Order parameters calculated from the trajectory demonstrated that hydrocarbon chains are more ordered in IAMs compared to fluid membranes. Collectively, these results suggest that the polar interfacial region of the IAM surface mimics well the polar interfacial region of fluid membranes, but the hydrocarbon part of the IAM surface has unique physicochemical properties compared to fluid membranes. The similarities between the physicochemical properties of IAMs and fluid membranes at the membrane interface explain, in part, why IAMs can be used to measure membrane partition coefficients for drugs and solutes.

Introduction

Immobilized artificial membranes (IAMs) are stable models of fluid membranes that can be used to rapidly evaluate drug−membrane interactions.[1,2] The ability of IAMs to accurately evaluate drug−membrane interactions was unexpected because IAMs contain immobilized phospholipids whereas fluid membranes are typically prepared from diacylated ester phospholipids. Furthermore, IAMs have been prepared from double chain ester PC analogs[3] or single chain ether PC analogs,[4] and for some IAMs the glycerol backbone has been removed.[1] In spite of these significant structural differences, all of the respective IAM surfaces accurately predict drug−membrane interactions.[1,5] This is highly unexpected when one considers both the structural and dynamic differences between immobilized lipids and fluid lipids. For IAMs to predict drug−membrane interactions, the IAMs must exhibit physicochemical properties similar to those of fluid membranes. The aim of our molecular dynamics simulation reported here was to identify common physicochemical properties between IAMs and fluid membranes. Many experimental[6−9] and theoretical[10−13] studies have increased our understanding of fluid membranes, but this is the first attempt at using MD simulations to explain the physicochemical properties of an immobilized artificial membrane system.

The primary structural feature of an immobilized artificial membrane (IAM) surface is a monolayer of membrane lipids with each lipid covalently immobilized to a mechanically stable matrix, e.g., to silica. Lipid immobilization during the preparation of IAMs eliminates molecular motions common to fluid membranes, i.e., flip-flop, lateral diffusion, axial displacement, etc. cannot occur. Furthermore, the immobilization process is expected to invert the motional gradient found in fluid membranes. In other words, IAMs are expected to have the greatest motion at the interfacial region and the least motion at the terminal part of the lipid alkyl chain. This is in contrast to fluid membranes that have the greatest molecular motion at the terminal part of the hydrocarbon chains because the nonbonded chains are free.

In addition to predicting the transport of solutes across biological barriers, IAMs have been used to purify several membrane proteins. IAMs have been used to purify phospholipase A2,[14] phosphatidylethanolamine-*N*-acyltransferase,[15] cholesterol−phospholipid transfer proteins,[16] several cytochrome p450 enzymes,[17] and a peptide transporter found in the Caco-2 cells.[18] The results from our MD simulation of an IAM surface

[⊗] Abstract published in *Advance ACS Abstracts,* June 15, 1995.

0022-3654/95/2099-11018$09.00/0

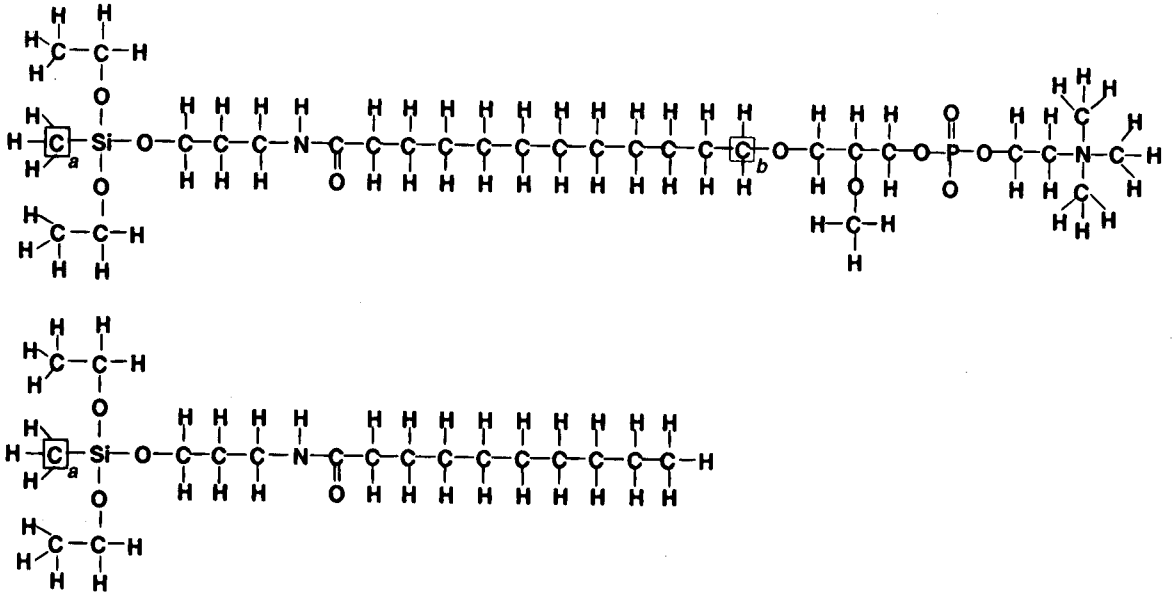

Figure 1. Chemical structures of phosphatidylcholine (PC) ligands and decanoyl ligands (C10) used to simulate the IAM surface. Silica propylamine is the matrix used to experimentally prepare IAMs. PC and C10 ligands are covalently linked to the silica propylamine functional groups through amide bonds. Typically, a triethoxysilane is used to prepare the silica propylamine. However, for the simulation, one of the ethoxy groups was replaced with a methyl group which was used as the "fixed" point for immobilization of the ligands to a surface. For all simulations C_a was fixed.

may provide insight into IAM surface chemistry that may allow a more efficient use of IAMs regarding the purification of membrane proteins.

Computer-Generated IAM Surface. The simulated IAM surface is similar to the experimentally prepared ^{ether}IAM.PC$^{C10/C3}$ surface. ^{ether}IAM.PC$^{C10/C3}$ was prepared by immobilizing *O*-[1-*O*-(11-carboxylundecyl)-2-*O*-methyl]-*sn*-3-glycerolphosphocholine (PC) on silica propylamine followed by end capping residual amines with decanoyl (C10) groups and then proprionyl (C3) groups.[4,19] Complete synthetic details for several IAM surfaces have been described.[4,19] All of the lipid ligands (PC, C10, and C3 groups) are linked to the silica surface through amide bonds.

The structures of the PC and C10 ligands used to simulate the IAM surface are shown in Figure 1. C3 alkyl groups were not included in the simulation because they are not expected to participate in solute binding to IAMs. Silica propylamine is the solid matrix used for immobilization of the lipid ligands. Although silica propylamine contains triethoxy groups in the experimental system, one of the ethoxy groups was converted into a methyl group; the carbon atom of this CH_3 group is denoted as C_a. Throughout the equilibration and simulations described below, the C_a group was immobilized. Thus, the C_a atom serves as the "fixed" immobilization point for the PC and C10 ligands shown in Figure 1.

An all-atom representation of the PC and C10 ligands was constructed using the *ChemNote* program found in *Quanta*.[20] Both atom types and partial charges for the PC and C10 atoms were provided by *ChemNote*. The bonded and van der Waals interaction parameters were taken from *Quanta's* parameter set and from the parameter file parallh22x.lip found in XPLOR. Water solvating the IAM surface was modeled using the TIP3 model.[21]

Experimentally, the molar ratio of PC and C10 groups on the IAM surface is 127:28 and it is assumed that the ligands are both randomly and uniformly distributed.[4] The experimentally measured density of immobilized PC molecules on the IAM surface is ~55−90 Å^2/molecule which indicates that 36 PC molecules and 7 C10 molecules occupy a total area of 1980−3240 Å^2. The simulated IAM surface patch was generated using these parameters. The random immobilization points for the C_a atoms, of both the PC and C10 ligands, were identified using

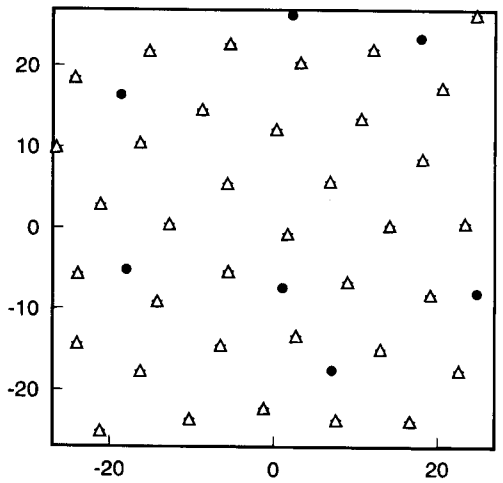

Figure 2. The ligand attachment points in the IAM unit cell. Attachment points are denoted as △ for PC ligands and ● for C10 ligands. The matrix represents the *x,y*-plane of the square IAM unit cell that is 54 Å × 54 Å.

the following procedure. The 36 PC molecules were represented using 36 point charges Q_1(=5) and the 7 C10 molecules using point charges Q_2(=1). Initially, the Q_1 and Q_2 charges were randomly placed in a 54 Å × 54 Å square. Repulsive Coulomb interactions between Q_1 and Q_2 were calculated using two-dimensional periodic boundary conditions. The positions of Q_1 and Q_2 were systematically reduced to minimize the total Coulombic interaction in the system. Since the Q_1 charges were 5 times the Q_2 charges, the Q_1 charges occupied a larger area in the final matrix. Energy minimization of the two-dimensional Q_1 and Q_2 charges gave the final positions of Q_1 and Q_2 in the matrix. Figure 2 shows the final distribution used to immobilize the C_a atoms of PC or C10 ligands. The PC and C10 ligands were oriented with the long axis of the molecules projecting out of the plane of the matrix shown in Figure 2, the latter direction being the *z*-direction for the simulation.

The *ChemNote*-generated structures for all PC and C10 ligands tethered to the matrix as shown in Figure 2 exhibited an unrealistic all-trans conformation. This extended alkyl chain conformation does not represent lipids in a thermally equilibrated

membrane. Since MD simulations can only be performed over very short time periods (picoseconds to nanoseconds), it is essential that the initial IAM system be thermally equilibrated prior to analyzing and interpreting atom trajectories. The IAM surface was equilibrated in two sequential steps using the boundary conditions described in the next section; however, a short Coulomb cutoff length (6−8 Å) was used to minimize the computation time required to equilibrate the system. Two-dimensional periodic boundary conditions (p.b.c.) in the x,y-plane were utilized during all equilibration steps and MD simulations. Although XPLOR only permits 3D periodic boundary conditions,[22] cutoffs in Coulomb interactions can effectively turn 3D p.b.c. into 2D p.b.c.; this is done by making the third dimension of the elementary cell (z-direction along the normal direction of the membrane) much longer than the Coulombic cutoff length so that neighboring two-dimensional x,y layers are uncoupled.

Two steps were used to equilibrate the IAM system. In the first step, the nonsolvated IAM surface was equilibrated at a high temperature, and in the second step a similar high-temperature equilibration was done in the presence of water. The following iterative procedure was used for the anhydrous high-temperature equilibration. The positions for all C_a and C_b atoms in both PC and C10 ligands (Figure 1) were fixed, and then MD simulations were performed at 400−1000 K for 1 ps. After the 1 ps simulation, the distance between C_a and C_b was decreased by δh (=0.2 Å) and the 1 ps simulation repeated. The process of decreasing the distance between C_a and C_b by δh followed by a 1 ps simulation was repeated until the final distance between C_a and C_b was 17.6 Å. The initial 27.4 Å thickness of the IAM surface (measured from phosphorous to C_a) was 22.8 Å after this initial high-temperature equilibration procedure.

The partially equilibrated IAM surface was solvated with ~2500 water molecules. A 31 Å slab of bulk water was overlaid on the partially equilibrated IAM surface such that the water slab begins near the glycerol ether oxygens of the PC ligands. For the simulation, $-z$ corresponds to the location of the C_a atom shown in Figure 1 and $+z$ corresponds to the outermost water molecules. The oxygen atoms of the water molecules within 3 Å from $+z$ were fixed to their original positions throughout all simulations. However, in contrast to fixing the C_b atoms during the high-temperature equilibration of the nonsolvated IAM surface, the C_b atoms were not fixed during the high-temperature equilibration of the solvated IAM surface. Thus, the C_b atoms were permitted to randomly fluctuate in the presence of solvation water during the second equilibration step. The initial height h_i of the C_b atoms was measured,

$$h_i = z(C_b) - z(C_a) \tag{1}$$

followed by a 5 ps MD simulation at 300 K. Even though energetically unfavorable steric interactions were avoided in the initial placement of water, our procedure could not avoid also adverse electrostatic interactions such that some water molecules are expected, initially, to prefer moving into the energetically unfavorable hydrocarbon region. Accordingly, water molecules that entered the hydrocarbon region, i.e., below the glycerol ether atoms, were removed at this point and another 5 ps equilibration performed. The solvation process was assumed complete when the condition

$$|h_{i+1} - h_i| \leq 0.1 \text{ Å} \tag{2}$$

was obeyed. Approximately 10 iterations were needed to satisfy condition 2, and only 10 water molecules were removed from the hydrocarbon region throughout the equilibration process. After solvating the IAM surface an additional 30 ps MD simulation at 300 K was performed to ensure equilibration of the system. The equilibrated IAM surface is shown in Figure 3. We note that XPLOR does not allow NpT ensemble simulations,[22] and consequently solvation of the IAM surface can not be done by merely adjusting the dimensions of the fundamental unit cell. The alternate method using a water slab placed on top of the IAM surface was needed.

The interconversion rates of trans−gauche conformers have a correlation time of about 25 ps for both immobilized PC and C10 ligands (see results section). Thus, the randomization/equilibration protocol described above required MD simulations for periods longer than 25 ps at room temperature. Alternatively, shorter equilibration periods at high temperature can be done. To a first approximation, the correlation time τ exhibits a strong temperature dependence described by $\tau \sim \exp(-\Delta E_b/k_BT)$ where ΔE_b is the energy barrier between trans and gauche configurations and T is temperature. The correlation time, thus, rapidly decreases with increasing temperature, and it is much more computationally efficient to randomize/equilibrate at high temperatures as was done for the IAM system.

Simulation Parameters. The partial charge assignments from *Quanta* were used for the PC and C10 molecules. The partial charge assignments from the topology file TIP3 were used for water. Coulomb interactions utilized a shifted potential

$$f_{\text{Coulomb}}(r) = Q_i Q_j \frac{1}{\epsilon_0 r}\left(1 - \frac{r^2}{r_{\text{off}}^2}\right)^2 \tag{3}$$

where the cutoff length was 6 Å during high-temperature equilibration steps and then 12 Å for the MD simulations. A switch function was used to cut off the van der Waals interaction

$$f_{\text{vdw}}(r) = \left(\frac{A}{r^{12}} - \frac{B}{r^6}\right)\text{SW}(r, r_{\text{on}}, r_{\text{off}}) \tag{4}$$

where the switch function is

$$\text{SW}(r, r_{\text{on}}, r_{\text{off}}) = \begin{cases} 0 & \text{if} \quad r > r_{\text{off}} \\ \dfrac{r^2 - r_{\text{off}}^2(r_{\text{off}}^2 - 3(r^2 - r_{\text{on}}^2))}{r_{\text{off}}^2 - r_{\text{on}}^2} & \text{if} \quad r_{\text{off}} > r > r_{\text{on}} \\ 1 & \text{if} \quad r < r_{\text{on}} \end{cases} \tag{5}$$

where r_{on} was 10 Å and r_{off} was 12 Å for all simulations. Equations of motion were numerically integrated using the Verlet algorithm and an integration time step Δt = 1 fs. Coordinate trajectories were saved every 500 fs.

Results and Discussion

The IAM system was constructed with the long axes of the immobilized lipids parallel to the z direction and the membrane interface residing in the x,y-plane. Both fluid and immobilized membranes contain a polar interfacial region and a nonpolar hydrocarbon environment. Extensive experimental work has been performed to elucidate the distribution of lipid functional groups across fluid bilayers,[8] but there are no reports of the functional group distribution across immobilized membranes. Consequently, the first comparison between IAMs and fluid membranes involved comparing the distribution of polar and nonpolar functional groups across each membrane. Interest-

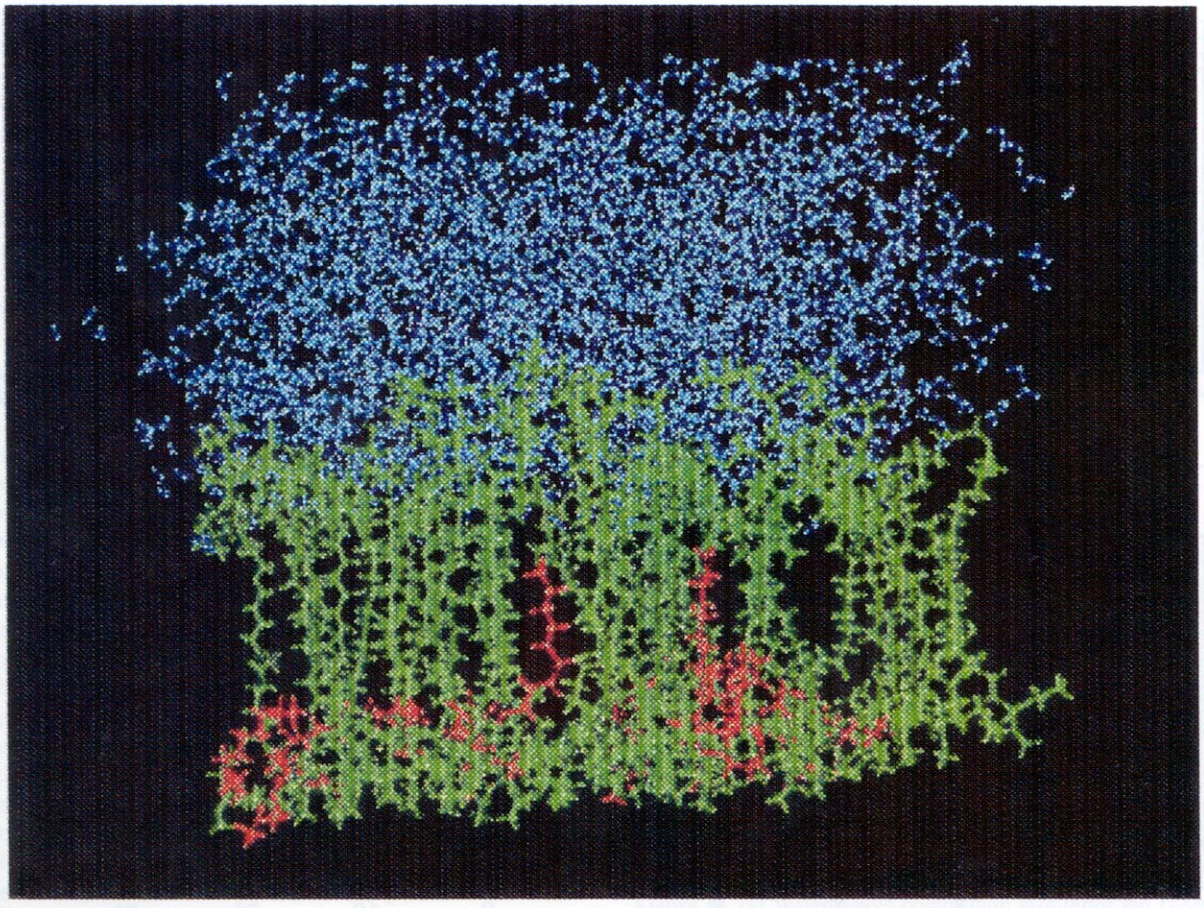

Figure 3. IAM structure after high-temperature equilibration and 250 ps of MD simulations.

ingly, the polar functional groups at the membrane interface may function as either a barrier to solute transport or as an adsorption site for solutes, and the distribution of functional groups at the membrane interface is responsible for these properties. A recent statistical mechanic theory has analyzed solute partitioning into bilayer membranes.[23]

Thirty-six PC molecules form the IAM surface in our simulation. We have determined the distribution $\varrho_\alpha(z)$ of functional groups α of lipids and the distribution of water. The procedure is best illustrated, for example, for phosphorus atoms. Thirty-six phosphorus atoms contribute to the distribution of this atom. During the 250 ps MD simulation, each phosphorus atom fluctuates and it was assumed for this atom and all other groups that the corresponding positions were Gaussian distributed. Accordingly, the total phosphorus distribution $\varrho_\alpha(z)$ was obtained by determining during the simulation the positions of the phosphorus atoms, drawing altogether, say, n samples. The Gaussian distributions for each phosphorus atom position z_i were added and normalized to obtain the total phosphorus distribution $\varrho_\alpha(z)$ using

$$\varrho_\sigma(z) = \frac{1}{\sigma n\sqrt{2\pi}} \sum \exp[-(z - z_i)^2/2\sigma^2] \qquad (6)$$

σ is the width of the Gaussian for which we assumed a value of 1.5 Å for all atom types and functional groups. The calculated atom distributions for functional groups associated with the PC ligand are shown in Figure 4a for the polar region (phosphate phosphorus, choline nitrogen, ether oxygen) and in Figure 4b for the nonpolar region (glycerol backbone carbons, hydrocarbon methylenes, ether *O*-methyl groups) of the IAM surface. The distribution of water at the IAM surface is also shown in Figure 4a. The distribution of water molecules shown in Figure 4b indicates that water did not penetrate into the hydrocarbon region of the IAM surface during the 250 ps simulation, and the peak intensity of the ether oxygen is larger than that of the other atoms because there are two ether atoms contributing to the distribution.

The glycerol backbone in membranes is the boundary between the polar interface and the nonpolar hydrocarbon environment of the lipid alkyl chains. For this reason, the position of the functional groups at the IAM surface was normalized relative to the average position of the glycerol backbone. For this calculation, the average position of the glycerol backbone itself was obtained from the total distribution of its three carbon atoms calculated according to (6). Relative to the glycerol backbone, the peak position and peak width in angstroms for the three polar functional groups shown in Figure 4a are

	ether oxygen	phosphate	choline nitrogen
peak position	−1.0 Å	3.5 Å	4.0 Å
peak width	5 Å	4.5 Å	7.0 Å

The peak positions characterize the average position of the atoms, but the peak widths are more indicative of the interfacial atom distribution in the z-direction. The peak widths for the phosphorus and oxygen atoms are similar (~5 Å), but the choline nitrogen has a large peak width of 7 Å. This indicates that the choline nitrogen exhibits the largest amount of fluctuation at the membrane interface compared to that of the other polar atoms.

Figure 4b shows the distribution of atoms comprising the nonpolar part of the IAM surface. As expected, the *O*-methyl group of the glycerol backbone exhibits virtually the same peak position and peak width compared to the glycerol backbone

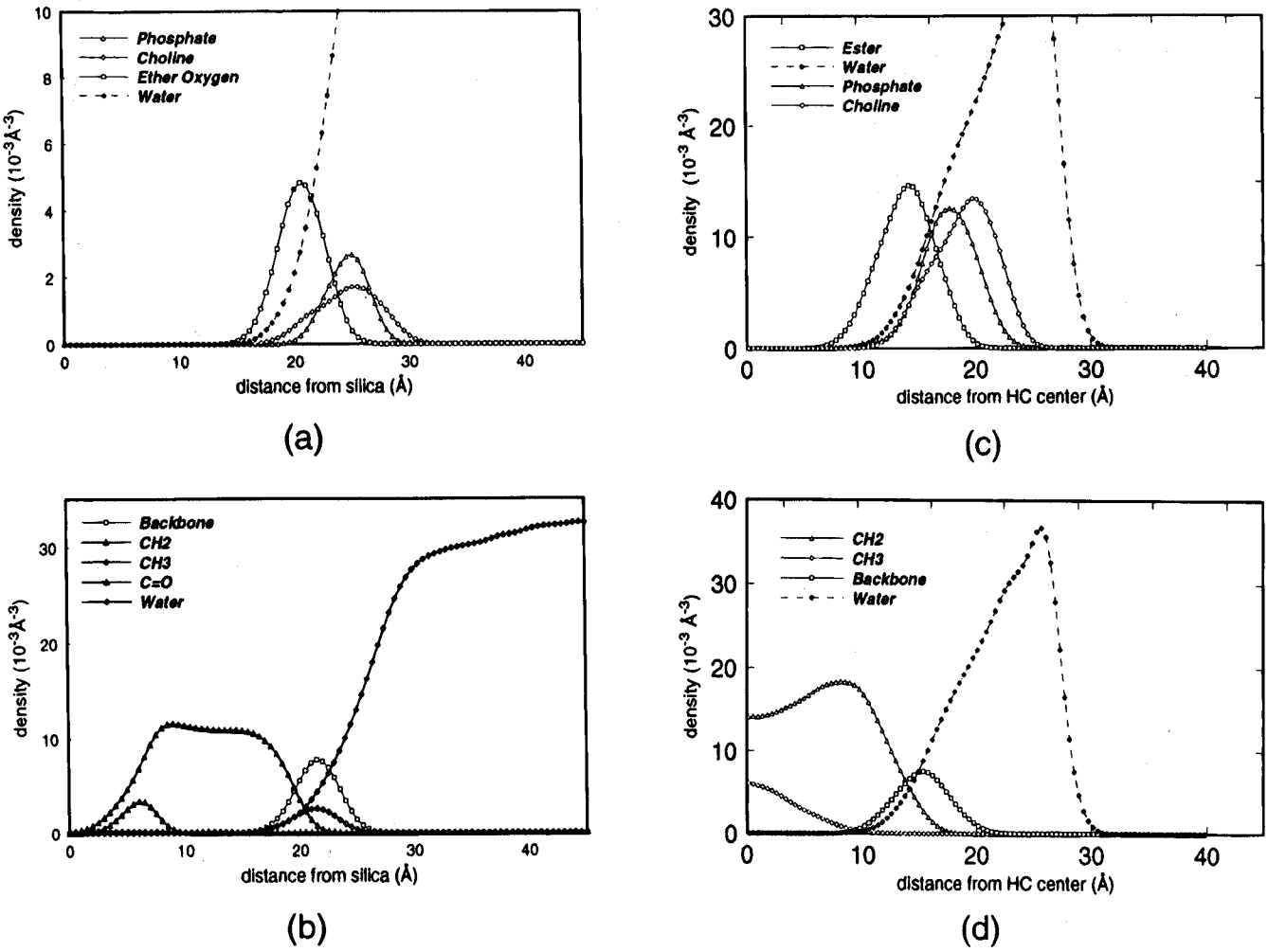

Figure 4. (a) Functional group distribution at the IAM interfacial region for the polar atoms of the PC ligands. The distributions were calculated from a 250 ps MD simulation using 500 trajectory points (0.5 ps/data point). The distribution of water solvating the membrane interface is also plotted. (b) Functional group distribution in the IAM nonpolar region. The functional group distributions correspond to both the PC and C10 ligands. The distributions of the methylene CH_2 groups for both the PC and C10 ligands were combined into one distribution. The distributions were calculated from a 250 ps MD simulation using 500 trajectory points (0.5 ps/data point). As a reference position, the average position of the glycerol backbone is plotted. For the glycerol backbone distribution, the three glycerol carbons were included in the same distribution and the curve shown reflects the average position for the entire glycerol backbone. In addition, the distribution of water at both the interfacial region of the membrane and bulk water is presented. (c) Functional group distributions of the polar atoms of the PC ligands forming a POPC bilayer membrane. The distributions were obtained from a previous MD simulation.[12] (d) Functional group distributions of the atoms in the nonpolar hydrocarbon region of POPC bilayer membranes. The distributions were obtained from a previous MD simulation.[12] For comparison, the distribution of the glycerol backbone is given.

carbons (parts a and b of Figure 4). The distribution of methylene groups on the IAM surface resides entirely between the amide bond ($z = 7$ Å) that links the PC ligand to the silica surface and to the glycerol backbone carbon atoms ($z = 21$ Å).

Figure 4c shows the distribution of polar functional groups at the membrane interface for fluid membranes prepared from 1-palmitoyl-2-oleyl-*sn*-3-glycerolphosphocholine.[8] This distribution was obtained from an MD simulation of POPC membranes,[12] which correlates well with X-ray data.[8] Similar to IAM membranes, the glycerol backbone (Figure 4d) was used as the reference point for comparing the positions of the polar functional groups. The peak position and standard deviations for the interfacial functional groups between immobilized and fluid (Figure 4) membranes are compared in Figure 5. Based on the distance between the polar atoms comprising the IAM surface and the surface of fluid PC membranes, IAMs are virtually identical to the POPC fluid membrane. The mean positions of the atoms and the amount of fluctuation in the positions (compare the standard deviations in Figure 5) are virtually identical between IAMs and fluid POPC membranes

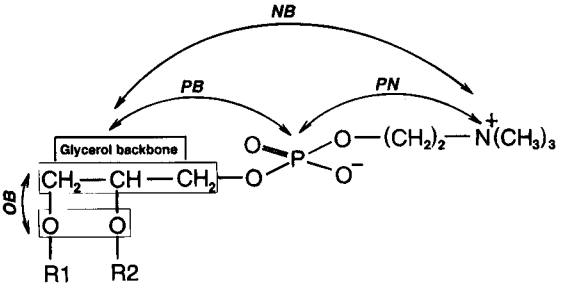

IAM		POPC	
Δh(PB) = 3.5 Å	Δw(P) = 4.5 Å	Δh(PB) = 2.5 Å	Δw(P) = 5.8 Å
Δh(PN) = 0.5 Å	Δw(N) = 7.0 Å	Δh(PN) = 1.9 Å	Δw(N) = 7.2 Å
Δh(NB) = 4.0 Å	Δw(GB)=5.0 Å	Δh(NB) = 4.4 Å	Δw(GB)= 5.5 Å
Δh(OB) =-1.0 A	Δw(O) = 5.0 Å	Δh(OB) =-1.2 Å	Δw(O) = 5.6 Å

Figure 5. Comparison of peak positions and half-peak widths for atoms at the membrane interface of immobilized membranes and fluid membranes. The peak positions were obtained from Figure 4a,b for IAMs and Figure 4c,d for POPC membranes.

for the phosphate, choline, and glycerol functional groups. Furthermore, the choline groups exhibit the largest motional fluctuations compared to phosphate groups, and this was also found during the simulations of both IAMs and POPC membranes. Finally, the distribution of water near the PC head groups in both the IAM and POPC membranes is the same; the solvation level ends at the C1 carbon of the glycerol backbone, and water does not penetrate into the hydrocarbon region of the membrane. However, for the IAM simulation, the orientation of the P−N vector is slanted approximately 3° relative to the membrane surface, whereas for fluid membranes a value near 17° is expected, based on NMR and X-ray diffraction studies.[24]

Water Polarization and Diffusion. The polar head groups of PC lipids have electric dipole moments pointing from the positive choline group to the negative phosphate group. Aside from being partially responsible for the intermolecular interactions between neighboring PC molecules, the head group dipoles also polarize water molecules that hydrate the interfacial choline phosphate groups. Water polarization refers to nonrandom water orientation near PC head groups. Nonrandom water orientation is the result of dipole−dipole interactions between the choline−phosphate dipoles and water. One expects that water molecules near the phosphate group orient in parallel with the water hydrogens facing the phosphate; on the other hand one expects that water molecules near the choline nitrogen are oriented in parallel with the water oxygen atoms facing the nitrogen atom. To quantitate water polarization at membrane interfaces, the magnitude of the water dipole moment was calculated as the sum of the O−H moments in the water molecule.

Figure 6a shows the water polarization profile across the entire z dimension of the IAM unit cell which includes both the hydrocarbon region and the polar region of the IAM system. The individual x, y, and z components of the water dipole moment are plotted to demonstrate that there is virtually no water polarization in the x,y-plane of the membrane but that there is a large water moment in the $+z$-direction. Most interestingly, the maximum water polarization (at ~23 Å) corresponds very closely to the midpoint of the P−N vector located at ~24.8 Å (Figure 4). On both sides of the maximum water polarization position at 23 Å, water polarization rapidly decreases, but the decay is linear toward the hydrocarbon region and exponential toward bulk water. The characteristic length over which the polarized dipole moment decreases to 1/e of its maximum strength is ξ = 13.2 Å which corresponds to an interfacial thickness of about four water molecules.

Because water polarization was both intense and very anisotropic near the membrane interface, we speculated that the diffusion of water molecules in this region may be anisotropic as well. Water diffusion at the membrane interface was calculated from the mean-squared displacements, using the relation

$$\lim_{t\to\infty} < \Delta r_i^2(h,t) \geq 2D_i(h)t \qquad (7)$$

where h is the distance of the water molecules from the bottom of the unit cell, $i = x$, y, or z indicates the three orthogonal directions, $\Delta r_i(h,t)$ is the displacement along the ith direction at time t, and $D_i(h)$ is the diffusion constant along ith direction. The calculated x, y, and z components of water diffusion are shown in Figure 6b.

Two regions of interest exist for the diffusion of water in the IAM system, and the regions are partitioned on either side of the 24 Å peak position of the water polarization profile shown in Figure 6a. The first region contains water molecules with a

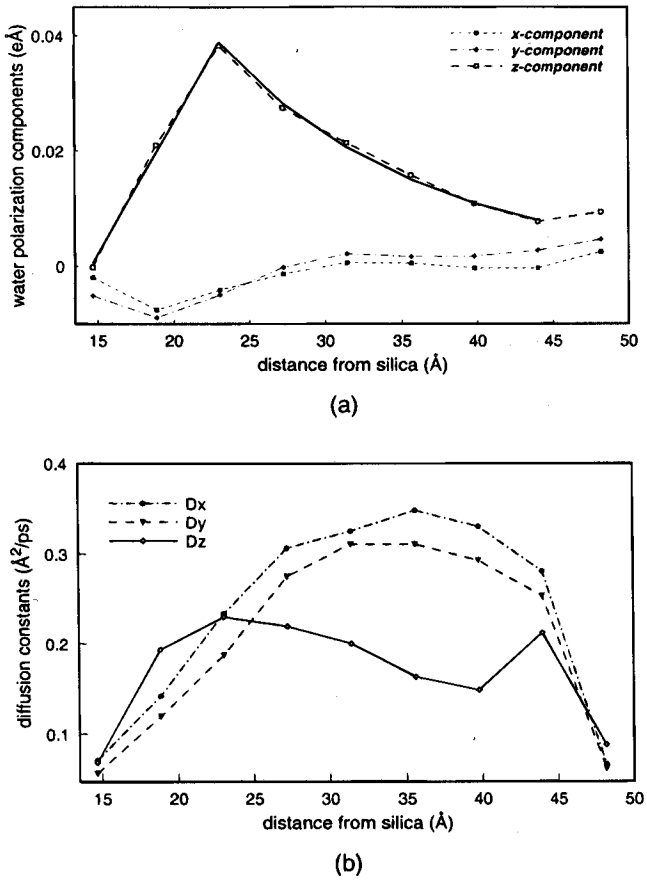

Figure 6. (a) Water dipole polarization profile for the IAM system using trajectories from a 250 ps MD simulation. Water did not penetrate the hydrocarbon region of the membrane and, therefore, the polarization profile begins near the glycerol backbone residing ~15 Å from the silica surface. The peak polarization occurred at 23 Å. The z-component of the water polarization profile was fit to an exponential function $f(h) = 3.08e^{-z/\xi}$ (ξ = 13.2 Å) in the range $z \in [23,45]$. (b) Water diffusion profile calculated from trajectories over 250 ps. The x-, y-, and z-components of water diffusion coefficients are shown. The glycerol backbone resides at ~15 Å, and the outermost water molecules reside at ~49 Å.

similar diffusion constant in all directions, and this is found for water molecules located at 15−24 Å in the z-direction (Figure 6b); this corresponds to the glycerolphosphocholine region of the IAM surface. This region contains only hydration water which solvates the PC head group. In this region, water diffusion is the slowest (~0.08 Å ^{2}/ps) for the few water molecules residing near the glycerol backbone, but water diffusion increases to ~$^1/_2$ of that found in bulk solution (0.36 Å^2/ps) for water molecules hydrating the choline N-methyls.

The second region of interest represents water molecules located in the range 24−45 Å, but the water diffusion data shown in Figure 6b for z > 45 Å are altered due to the boundary region in which the water molecules were immobilized. Nevertheless, the 24−45 Å region corresponds to water molecules in the outermost hydration layer of the PC head groups and also to bulk water. The general features for water diffusion in this region are: (i) similar water diffusion constants are found in the x and y directions: (ii) water diffusion in the z-direction is 50 % slower. The D_x and D_y components of water diffusion range from 0.31 to 0.35 Å^2/ps, and this value is close to the 0.36 Å^2/ps diffusion constant found in bulk water.[10,21] Water diffusion in the z-direction ranges from 0.15 to 0.22 Å^2/ps which is 50 to 33% less than the diffusion coefficient of bulk water. The physical significance of the water diffusion

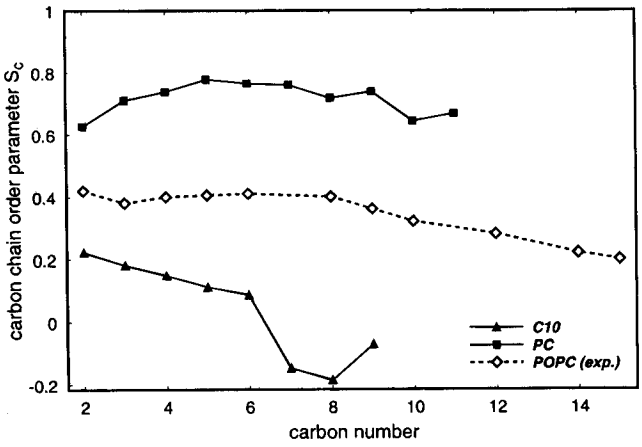

Figure 7. Carbon chain order parameters for hydrocarbon chains in both PC and C10 molecules. The experimentally measured order parameters for the saturated chain in a POPC liquid bilayer[27] are also plotted for comparison.

profiles shown in Figure 6b is that the interfacial water molecules rapidly diffuse parallel to the membrane interface in the x,y directions, but water diffusion away from and toward the membrane interface is relatively slow. Water molecules are highly polarized as they approach the lipid head groups. This induced polarization coupled to the requirement for an incoming water molecule to displace a hydration water molecule apparently limits the rate of water diffusion normal to the membrane interface.

The functional group distributions in parts a and b of Figure 4 demonstrated that water did not diffuse into the hydrocarbon region of the IAM interphase during the 250 ps simulation. This is consistent with the smallest water diffusion constants found near the glycerol backbone at 15 Å; this entry point for water to enter the hydrocarbon region creates an environment such that water molecules exhibit a diffusion constant of only 0.08 Å^2/ps. During the 250 ps simulation, water molecules can travel 6 Å, but both slow diffusion and water polarization prevent water from penetrating into the IAM hydrocarbon region.

Hydrocarbon Chain Order Parameters and Trans–Gauche Interconversion Rates. In fluid membranes reorientation of individual methylene groups depends on the position of the methylene groups in the membrane. The disorientation of particular methylene groups at a particular depth in the bilayer is calculated as an order parameter labelled S_c. The order parameter provides a measure for the average position away from the membrane normal for each methylene group. The order parameters along the hydrocarbon chain are calculated from

$$S_c(n) = \frac{1}{2}[3 \cos \theta_z(n) \cos \theta_z(n) - 1] \qquad (8)$$

where $\theta_z(n)$ is the angle between the membrane normal and the vector from $C_{(n-1)}$ to $C_{(n+1)}$. S_c equals 1 for the all-trans configuration oriented parallel to the membrane normal, and S_c equals $-1/2$ for an all-trans configuration oriented perpendicular to the membrane normal. Completely randomly oriented alkyl chains have $S_c = 0$. Order parameters for the methylene groups in both PC and C10 for both the immobilized membrane and fluid POPC membrane are shown in Figure 7. As expected for fluid membranes, the methylene order parameters are ~0.4 for the first 4–6 PC methylene groups, but for methylene groups residing at positions 8–14, the order parameters linearly decrease (Figure 7). Compared to fluid membranes, all of the methylene groups in immobilized PC molecules are more ordered. This is apparent in Figure 7 which shows that the PC molecules have 50–100% higher order parameters. In contrast to immobilized PC, immobilized C10 are much more disordered compared to the alkyl chains in fluid membranes. This is apparent in Figure 7 which shows that the order parameters for methylene groups in C10 have at least 50% lower order parameters. More importantly, the order parameters near the end of the floppy chain are less than zero, which suggests that this segment of the C10 group lies approximately parallel to the membrane surface. As shown in Figure 3, several of the C10 ligands have come to rest on the floor of the silica, which corresponds to a molecular orientation that is parallel to the membrane interface. Thus, the order parameters calculated in Figure 7 are consistent with the 250 ps MD simulation.

Order parameters calculated according to eq 8 are relative to the membrane normal, and this creates a problem for analyzing immobilized membranes that contain a few C10 ligands lying on the silica surface. C10 ligands lying on the floor of the silica surface during the 250 ps MD simulation (Figure 3) are oriented parallel to the membrane normal, and this results in a very low order parameter calculated from eq 8. However, if the methylene groups in the C10 ligands contain a large fraction of trans conformers, then the C10 ligands are actually highly ordered and may be considered as alkyl chain rods lying on the floor of the IAM surface. Thus, it is possible to have rigid extended alkyl chains parallel to the membrane surface with a low order parameter calculated by eq 8, but the true configurational entropy is quite low because the molecule is like a rod with all of the methylenes in an all-trans configuration. Equation 8 alone can not adequately describe the amount of segmental order for the molecules comprising the IAM surface. Consequently, we evaluated the ratio of trans:gauche methylene conformers because this is a direct measure of chain disorder; the number of trans–gauche conformers was calculated for the methylene groups of the IAM surface.

The distributions of dihedral angles $P(\cos \phi)$ for the C10 methylenes and PC methylenes are plotted in Figure 8a. The logarithmic scale for $P(\cos \phi)$ emphasizes the distribution around the gauche configurations. Trans dihedral angles correspond to $\phi = 180°$ ($\cos \phi = -1$), and gauche dihedral angles correspond to $\phi = \pm 60°$ ($\cos \phi = 0.5$). The percentages of trans and gauche configurations are obtained by integrating the probability distribution $P(\cos \phi)$ between $\cos \phi \in [-1, -0.5]$ and $\cos \phi \in [-0.5, 1]$, respectively. The trans–gauche ratio is 0.84:0.16 for PC molecules and 0.68:0.32 for C10. Most interestingly, this ratio corresponds very well to the theoretical ratio based on Boltzmann statistics using the energy associated with conformationally unrestricted alkyl chains. Theoretically, a hydrocarbon chain, all segments of which can freely move, has a ratio of trans to gauche dihedral angles related to the energy barrier $\Delta E = 0.7$ kcal/mol associated with the rotational interconversions of trans–gauche conformers. At $T = 300$ K, the trans–gauche conformer ratio of a floppy chain in a fluid membrane can be calculated from Boltzmann statistics as

$$\text{trans:gauche} = (1 - e^{-\Delta E/(k_B T)}):\ e^{-\Delta E/(k_B T)} = 0.69:0.31 \qquad (9)$$

and this ratio of 0.69:0.31 is very close to the ratio obtained for the immobilized C10 chain where the trans–gauche ratio was 0.68:0.32 after the 250 ps MD simulation. Most interestingly, the immobilized PC ligand which contains a bulky head group had a trans:gauche ratio of 0.84:0.16 after the 250 ps MD simulation, and this is not close to the theoretical value predicted by eq 9. Thus, tethering a PC molecule to the silica surface (but not the C10 molecules to the silica surface)

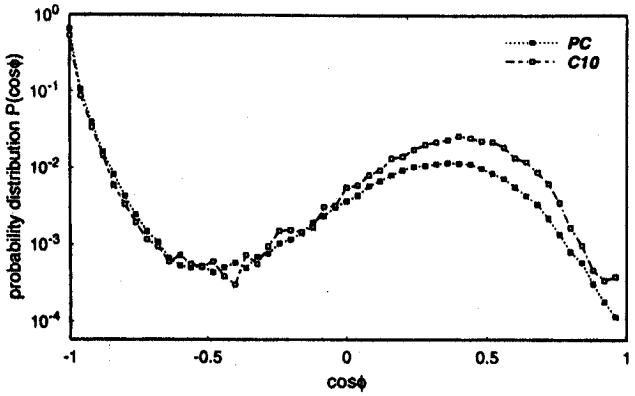

(a)

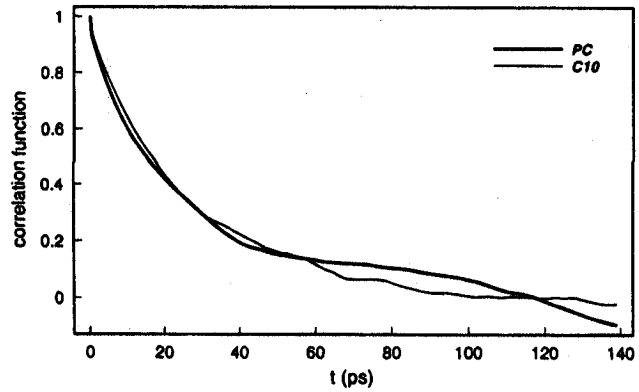

(b)

Figure 8. (a) Probability distributions of cos ϕ, where ϕ is the dihedral angle formed by neighboring carbon atoms in the hydrocarbon chains of PC and C10 molecules. (b) Correlation function $C_\phi(t)$ of the dihedral angles throughout the lipid alkyl chains of the PC and C10 immobilized ligands. The correlation time τ_c obtained from an exponential fit of the curves was ~25 ps for both PC and C10 molecules.

significantly increases the energy barrier to rotational interconversion of the trans–gauche methylene conformers. This is most likely due to (i) anchoring the PC ligand to the silica surface and (ii) a bulky PC head group. Both of these factors contribute to the restriction of the alkyl chain of the immobilized PC ligand but do not restrict the chains of the immobilized C10 ligands. In fluid membranes, the alkyl chains are free to rotate independently of the PC head group because the terminal part of the alkyl chains is not immobilized as in the IAM system.

In addition to characterizing the static population of trans–gauche conformers, the interconversion rates between trans–gauche conformers provide another important characterization of membrane alkyl chains. The transition time between trans and gauche configurations in fluid membranes is on the order of picoseconds. The transition time between trans–gauche interconversions was determined by calculating the normalized dihedral correlation function

$$C_\phi(t) \equiv \frac{\langle \cos\phi(t)\cos\phi(0) - \cos\phi(\infty)\cos\phi(0)\rangle}{\langle \cos\phi^2(0) - \cos\phi(\infty)\cos\phi(0)\rangle} \quad (10)$$

where $\langle ... \rangle$ indicates the ensemble average. Assuming the correlation function decays exponentially with time, the correlation time τ of the dihedral interconversions can be obtained by matching (10) to the function

$$C_\phi(t) = e^{-t/\tau} \quad (11)$$

The dihedral correlation functions for PC and C10 molecules shown in Figure 8b exhibit nearly the same correlation times, namely,

$$\tau_{PC} \approx \tau_{C10} \approx 25 \text{ ps} \quad (12)$$

These trans–gauche interconversion rates of methylenes in the hydrocarbon part of immobilized membranes are ~25-fold slower than the same fluctuations in fluid membranes.

Phosphate Group Diffusion. The interfacial properties of IAMs have been studied by ^{31}P NMR line shape analysis and T_1-relaxation measurements.[25,26] The immobilized ligands on the IAM surface cannot undergo lateral diffusion or axial displacement and, therefore, a pure rotational diffusion model was used for the ^{31}P NMR analysis of IAMs. Immobilized phospholipid ligands can "wobble" in the plane of the membrane or undergo internal reorientation from bond rotations. With regard to rotational diffusion of the phospholipid head group, conformational changes in the C–C glycerol backbone bonds and rotations in the glycerol–phosphodiester P–O bonds significantly contribute to the head group motion. The P–O glycerol–phosphodiester bond is assumed to be the z'-axis for the NMR analysis, and rotation was assumed to be symmetric about this axis.[25,26] Two diffusion constants were calculated from the MD simulation: d_{zz} is the rapid reorientation of the phosphate around the z'-axis and d_{xy} is the diffusion constant corresponding to reorientation in the plane of the membrane due to wobbling. Both d_{xy} and d_{zz} have been determined by line shape analysis of ^{31}P data of IAMs.[25,26]

The trajectory of phosphate groups during the 250 ps simulation of the IAM surface was analyzed to obtain simulated values for d_{zz} and d_{xy}. The correlation time for phosphate group wobbling in the plane of the immobilized membrane was calculated from

$$C_\theta(t) = \langle [\theta(t) - \theta(0)]^2 \rangle = 2D_\theta t \quad (t \to \infty) \quad (13)$$

where θ is the angle measured from the phosphate z'-axis to a line normal to the IAM surface. The correlation times for the phosphate group undergoing internal rotations were calculated from

$$C_\phi(t) = \langle [\phi(t) - \phi(0)]^2 \rangle = 2D_\phi t \quad (t \to \infty) \quad (14)$$

where ϕ is the reorientation angle corresponding to rotation around the P–O bond in the glycerol–phosphodiester linkage. Linear regression in the domain $t \in (40,150)$ ps of the correlation functions corresponding to d_{xy} and d_{zz} in Figure 9 was used to calculate the correlation times τ_c associated with slow head group wobbling and rapid head group internal rotation. The rapid internal rotational diffusion coefficient, experimentally measured by ^{31}P NMR spectroscopy, was $d_{zz} = 1$ ns^{-1} which is quite close to the value d_{zz} (=D_ϕ) = 1.7 ns^{-1} obtained from our 250 ps MD simulation. However, the slow head group wobbling motion, calculated from the 250 ps MD simulation, gave the value of $d_{xy} = 0.5$ ns^{-1} which is 10^2 faster than the ^{31}P NMR determined value of $d_{xy} = 0.0001$ ns^{-1}. Thus, the 250 ps MD simulation was able to characterize rapid internal rotation of the phosphorus atom at the interface but not the slow wobbling motion. Since it is unrealistic to expect a 250 ps MD simulation to accurately characterize motion that exhibits a correlation time of microseconds, an explanation for the lack of correlation between d_{xy} values between simulated and ^{31}P NMR is unnecessary.

Equilibration of the IAM System. For any MD simulation the extent of system equilibration is always questioned. One measure of the extent of the equilibration of the IAM system is

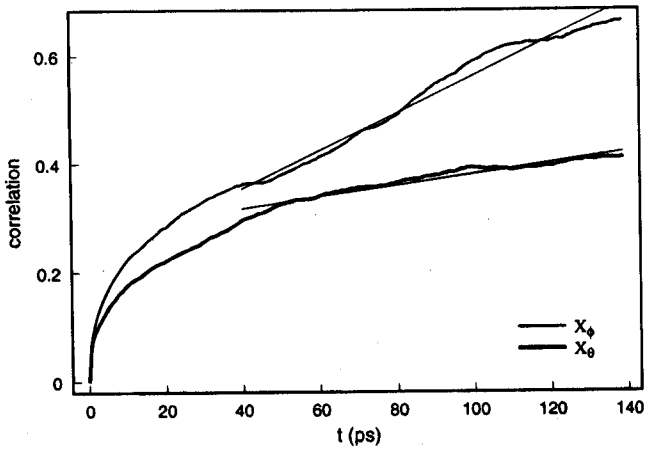

Figure 9. Correlation functions for phosphate group reorientation calculated from the positional fluctuations of the phosphorus atom during a 250 ps MD simulation of the IAM surface. The straight lines represent the linear regression analysis used to obtain diffusion constants $D_\theta = 0.5$ (ns^{-1}) and $D_\phi = 1.7$ (ns^{-1}).

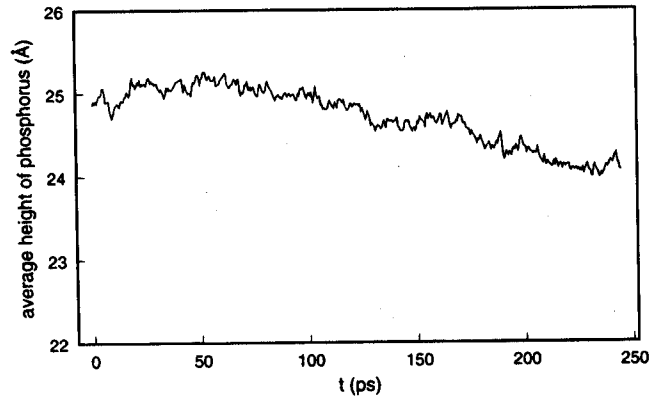

Figure 10. Average position of the phosphorus atom during a 250 ps MD simulation.

to evaluate if the phosphorus atom does not change its average position in the plane of the membrane during the simulation. In other words, if the system is equilibrated, then the thickness of the immobilized layer of lipids does not change and the average position of the phosphate, choline, etc. does not change. Thus, the key question for our MD simulation is, "Does the thickness of the lipids remain constant during the simulation?" Figure 10 presents the average height of the phosphorus atom as a function of simulation time. The average phosphorus height decreases by about 0.6 Å during the 250 ps simulation; this indicates that the IAM surface is slightly thinning. However, a 0.6 Å thinning of the monolayer should be compared to the 4.6 Å decrease in the monolayer that occurred during the high-temperature randomization/equilibration of the IAM system. A thinning of 0.6 Å during the simulation is approximately 13% of the monolayer thinning experienced during the randomization/equilibration process, and this indicates that the IAM system used for our studies is well equilibrated.

After any membrane perturbation, complete membrane relaxation requires longer than 1 ns which is 1000 times slower than the calculated correlation times for trans–gauche interconversions, phosphorus reorientation diffusion rates, water diffusion rates, etc. during the 250 ps MD simulation of the IAM surface. Thus, the IAM system is essentially static (i.e., equilibrated) during the sampling of the individual atom positions throughout the 250 ps trajectory. If the dynamic process associated with the IAM surface had relaxed on a very long time scale, then insufficient sampling would have occurred, but this is not the case for our system.

Summary

MD simulations demonstrated that the average position of the phosphate, choline, glycerol backbone, and ether/ester oxygens in the IAM interfacial region is similar to the average position of these functional groups found in fluid POPC membranes. Water does not penetrate into the hydrophobic region of either IAM or POPC membranes. Water is distributed at the IAM interface with vanishing density at the hydrocarbon region, with a low density at the glycerol backbone, and with a bulk water density at ~10 Å from the glycerol backbone. Water diffusion in the glycerolphosphocholine region of the membrane is isotropic in the x,y-plane of the membrane but anisotropic in the z-direction. The diffusion of water along the membrane normal direction is ~50% slower than diffusion parallel to the membrane interface. One factor contributing to this anisotropy of water diffusion is the anisotropic polarization in the water dipole induced by the electric dipole of the PC headgroups. The highly polarized water molecules at the polar interfacial region of the IAM membrane shield the potential generated by the head group dipoles. The water polarization profile decays exponentially toward bulk water with a decay length of ~13 Å, i.e., about four water molecules.

PC hydrocarbon chains in the IAM are more ordered compared to the hydrocarbon chains found in POPC fluid bilayers. In fluid membranes the alkyl chains are free to rotate, independent of the lipid headgroups, but this is not the case when PC lipids are tethered to a solid surface. However, compared to the amphipathic immobilized PC ligand, the completely hydrophobic immobilized C10 ligand freely moves in the IAM system. This suggests that anchoring the ligands themselves to the surface is not the only limitation in configurational entropy, but also the hydrophobic–hydrophilic nature of the immobilized ligand controls, in part, the interaction energy between neighboring ligands.

The simulation was intended to increase our understanding of the predictability of IAMs regarding solute partitioning into fluid membranes. A statistical mechanical theory has recently described the drug-partitioning process in fluid membranes,[23] and this theory has accounted for the interaction energies between solutes and fluid membranes. IAMs are good models of the solute-partitioning process, and the 250 ps MD simulation demonstrated that there are several common interfacial properties between IAMs and fluid membranes. The observation that IAM surfaces have similar physicochemical properties compared to fluid membrane bilayers at the interfacial region corroborates the hypothesis that IAM surfaces can predict drug partitioning and drug transport in fluid membranes.

Acknowledgment. We thank Tom Bishop, Bill Humphrey, and Ilya Logunov for their help on some technical problems in our simulations. One of the authors (Q.S.) thanks Manel Balsera and Professors Eric Jakobsson and Shankar Subramaniam for many useful and intriguing discussions. This work was carried out at the Resource for Concurrent Biological Computing funded by the National Institutes of Health (P41RRO5969). This work was also supported by Eli Lily and Company. C.P. is supported by NIH (AI 33031, 2R446M3022-02) and NSF (CTS 9214794).

References and Notes

(1) Ong, S.; Liu, H.; Qiu, X.; Bhat, G.; Pidgeon, C. *Anal. Chem.*, in press.

(2) Pidgeon, C.; Ong, S.; Liu, H.; Qiu, X.; Pidgeon, M.; Dantzig, A. H.; Munroe, J.; Hornback, W. J.; Kasher, J. S.; Glunz, L.; Szczerba, T. *J. Med. Chem.*, in press.

(3) Pidgeon, C.; Venkatarum, U. V. *Anal. Biochem.* **1989**, *176*, 36–47.

(4) Rhee, D.; Chae, W. G.; Qiu, X.; Pidgeon, C. *Anal. Chim. Acta* **1994**, *297*, 387−386.
(5) Ong, S.; Pidgeon, C. *Anal. Chem.*, submitted.
(6) Seelig, A.; Seelig, J. *Biochemistry* **1974**, *13*, 4830−4845.
(7) Seelig, J. *Q. Rev. Biophys.* **1977**, *10*, 353−418.
(8) Wiener, M. C.; White, S. H. *Biophys. J.* **1992**, *61*, 434−447.
(9) Paltauf, F.; Hauser, H.; Phillisps, M. C. *Biochim. Biophys. Acta* **1971**, *249*, 539−547.
(10) Egberts, E.; Berendsen, J. C. *J. Chem. Phys.* **1988**, *89*, 3718−3732.
(11) Curvin, M. S. *J. Phys. Chem.* **1985**, *89*, 4707−4713.
(12) Heller, H.; Schaefer, M.; Schulten, K. *J. Phys. Chem.* **1993**, *97*, 8343−8360.
(13) Cevc, G.; Marsh, D. *Phospholipid Bilayer: Physical Principles and Models*; Wiley: New York, 1987.
(14) Pidgeon, C.; Cai, S.; Bernal, C. *J. Chromatogr. A*, submitted.
(15) Cai, S.; McAndrew, R. S.; Leonard, B. P.; Chapman, K. D.; Pidgeon, C. *J. Chromatogr. A*, in press.
(16) Thurnhofer, H.; Schnabel, J.; Betz, M.; Lipka, G.; Pidgeon, C.; Hauser, H. *Biochim. Biophys. Acta* **1991**, *1064*, 275−286.
(17) Pidgeon, C.; Stevens, J.; Otto, S.; Jefcoate, C.; Marcus, C. *Anal. Biochem.* **1991**, *194*, 163−173.
(18) Pidgeon, C. Unpublished results.
(19) Ong, S.; Cai, S. J.; Bernal, C.; Rhee, D.; Qiu, X.; Pidgeon, C. *Anal. Chem.* **1994**, *66*, 782−792.
(20) *Quanta*; Polygen Corp.: Waltham, MA, 1988.
(21) Jorgensen, W. L.; Chandrasekhar, J.; Madura, J. D.; Impey, R. W.; Klein, M. L. *J. Chem. Phys.* **1983**, *79*, 926−935.
(22) Brunger, A. T. *X-PLOR A System for X-ray Crystallography and NMR*, Version 3.1; Yale University Press: New Haven and London, 1992.
(23) Xiang, T.; Anderson, B. D. *Biophys. J.* **1994**, *66*, 561−573.
(24) Seelig, J. *Biochim. Biophys. Acta* **1978**, *515*, 105−140.
(25) Qiu, X.; Pidgeon, C. *J. Phys. Chem.* **1993**, *97*, 12399−12407.
(26) Ong, S.; Qiu, X.; Pidgeon, C. *J. Phys. Chem.* **1994**, *98*, 10189−10199.
(27) Seelig, J.; Seelig, A. *Q. Rev. Biophys.* **1980**, *13*, 19−61.

JP950170B